HHS Public Access

Author manuscript

Neuron. Author manuscript; available in PMC 2017 February 03.

Published in final edited form as:

Neuron. 2016 February 3; 89(3): 629–644. doi:10.1016/j.neuron.2015.12.035.

Sensorimotor transformations underlying variability in song intensity during *Drosophila* courtship

Philip Coen[1], **Marjorie Xie**[1], **Jan Clemens**[1], and **Mala Murthy**[1,2]

[1]Princeton Neuroscience Institute, Princeton University, Princeton, NJ

[2]Department of Molecular Biology, Princeton University, Princeton, NJ

Summary

Diverse animal species, from insects to humans, utilize acoustic signals for communication. Studies of the neural basis for song or speech production have focused almost exclusively on the generation of spectral and temporal patterns, but animals can also adjust acoustic signal intensity when communicating. For example, humans naturally regulate the loudness of speech in accord with a visual estimate of receiver distance. The underlying mechanisms for this ability remain uncharacterized in any system. Here, we show that *Drosophila* males modulate courtship song amplitude with female distance, and we investigate each stage of the sensorimotor transformation underlying this behavior, from the detection of particular visual stimulus features and the timescales of sensory processing, to the modulation of neural and muscle activity that generates song. Our results demonstrate an unanticipated level of control in insect acoustic communication, and uncover novel computations and mechanisms underlying the regulation of acoustic signal intensity during communication.

Introduction

Adjustment of song or speech intensity is an important aspect of communication. Careful production of the correct frequency and phasic characteristics is useless if the acoustic signal either overwhelms the auditory system of the communication partner, or is too soft to be detected. During communication, acoustic signal quality typically decreases as the distance between sender and receiver increases. Humans naturally compensate for this by adjusting speech intensity when shouting across a room or sharing a conspiratorial whisper (Zahorik and Kelly, 2007). Despite the clear ethological relevance of adjusting for communication distance, outside of humans, this behavior has only been reported in songbirds (Brumm and Slater, 2006). Insects also use acoustic signals for communication, and some produce two different varieties, one for calling a distant partner and another for courting a nearby one

Correspondence: mmurthy@princeton.edu.

Author Contributions: PC and MM designed the study. PC MX and JC collected the data. PC analyzed the data and made the figures. PC and MM wrote the paper.

(Alexander, 1961). However, modulation of a single acoustic signal over a range of target distances has never been documented in invertebrates, likely due to experimental challenges (Chakravorty et al., 2014; Tauber and Eberl, 2001). *Drosophila* males produce a courtship song with large variations in amplitude over short timescales (tens of milliseconds) (Bennet-Clark, 1971). But speech or song **a**mplitude **m**odulation with **d**istance (AMD) requires not only the ability to vary acoustic signal amplitude, but also to accurately estimate target distance. Flies can use visual cues to identify the closer of two stationary targets while either walking or in flight (Schuster et al., 2002; Cabrera and Theobald, 2013). Furthermore, the choice of which courtship song mode to sing is based in part on the *Drosophila* male's distance to the female, which he measures using visual cues (Coen et al., 2014), suggesting that males can estimate distance even while the target is persistently translating and rotating. Combined, these studies indicate that flies exhibit the ethological motivation, computational capacity, and mechanical ability, to execute AMD. But do they?

For any animal to perform AMD, a sensorimotor transformation must take place within the nervous system, relaying information about the visual representation of the communication partner to motor pathways that generate dynamic acoustic signals. These transformations, in general, require 1) extracting the relevant features of the sensory stimulus, 2) processing sensory information on timescales appropriate for behavior, and 3) driving a specific change in motor output. Here, we address all three stages in *Drosophila*, using a combination of quantitative behavioral assays, statistical modeling, genetic mutations, electrophysiology, and neural circuit activation or silencing. We first establish that male flies perform AMD, and rely on vision to compensate for a range of female distances. We then determine the visual stimulus features required to estimate distance in this context and resolve the timescales over which visual information is processed. Additionally, we investigate the neural pathways that carry distance information and the point of intersection between visual processing and song motor circuits. Surprisingly, our results suggest that a single circuit independently regulates song amplitude and song timing — a mechanism likely to be generalizable, as effective communication relies on the ability to change the gain of an acoustic signal without altering its temporal structure. Finally, we implicate a specific subset of muscles in regulating song intensity. In sum, our data provide new insight into the sensorimotor transformation that underlies a fundamental, innate behavior performed by disparate animal species.

Results

Drosophila males compensate for distance to the female by modulating song amplitude

Drosophila melanogaster males vibrate their wings to produce a highly variable courtship song, comprising two primary modes—pulse trains and sinusoids (Coen et al., 2014) (Figure 1A). Males produce pulses over a broad range of amplitudes (Figure S1A), and unlike sinusoids, each pulse is a discrete event (akin to neural spikes). This facilitates the calculation of amplitude, timing (measured by the inter-pulse interval or IPI), and frequency for individual pulses. For these reasons, pulse trains are well suited to an investigation of amplitude modulation with distance (AMD) in *Drosophila*. We designed an assay that permits simultaneous tracking of fly position while recording courtship song in a large

behavioral chamber tiled with microphones (Coen et al., 2014) (Video S1). This setup allowed us to acquire a large sample of pulses over a range of inter-fly distances (up to 20mm or~8 body lengths). Further, we used tracking data to normalize recorded pulse amplitudes for both changes in male position and differences in microphone sensitivity (Figure 1B, and see Experimental Procedures)—not doing so can introduce artificial variations in recorded amplitude (Chakravorty et al., 2014; Tauber and Eberl, 2001). The dataset presented here comprises > 5 million song pulses. The fly strains used in this study, their acronyms, and any data that were previously published, are detailed in Table S1. Genotypes of fly strains are provided in the Experimental Procedures.

Because changes in wing size introduce systematic inter-fly variability in song amplitude (Figure 1C, black circles), we z-scored pulse amplitudes produced by each fly before combining data within a single strain or across strains. We did this because we wanted to determine whether males *change* their pulse amplitude with distance (i.e. perform AMD), while ignoring inter-fly differences in the distribution of pulse amplitudes. That is, z-scoring forces the amplitude distribution for each fly to have a mean of zero and a standard deviation of one—the “normalized amplitude” we report is thus defined by how much the amplitude of a pulse differs from the mean (zero). Although we also normalized for male position, and microphone sensitivity (see Experimental Procedures), male wing choice (singing with his left or right wing), which we did not score, still introduced variations in recorded amplitude and limited the significance of our results.

As an unbiased test for AMD, we utilized a generalized linear model (GLM) (Coen et al., 2014) to determine whether any features of the male’s sensory environment predicted the amplitude of individual pulses (Figure 1D). Unlike correlational analyses, the GLM we used included a sparsity prior, which disentangled the contributions of different sensory features (Mineault et al., 2009). We modeled data from 315 pairings of virgin flies from eight geographically diverse strains. Females were genetically engineered to be pheromone insensitive and blind (Coen et al., 2014). When we compared GLMs based on one of 9 features that describe the movement and relative position of both flies (Figure 1D inset), distance to the female (Dis) proved the strongest predictor of pulse amplitude. This remained true even when considering additional features such as fly acceleration and the subtended angle of the female on the male retina (Figure S2A). We repeated the model-selection process, combining Dis with each remaining feature, and found male forward velocity (mFV) to be a significant secondary predictor of pulse amplitude (Figure 1E). For these two features, we found that Dis and mFV were most predictive when delayed by ~470ms and ~100ms respectively (Figure 1F). For Dis, the broad peak and residual predictive power at pulse onset likely derive from the wide auto-correlation of this feature during natural courtship (Figure S2B). This may also explain the correlation between amplitudes of adjacent pulses (Figure S1B–C). Hereafter, features evaluated at a specific temporal delay are denoted by superscript (i.e. Dis^{470} for inter-fly distance at 470ms prior to the pulse and mFV^{100} for male forward velocity 100ms prior to the pulse). We found a strong correlation between Dis^{470} and amplitude for all wild type strains tested ($r^2 \geq 0.69$, Figure S2C), and for a closely related sibling species, *Drosophila simulans*, suggesting that AMD is evolutionarily conserved ($r^2 = 0.80$, Figure S2D). These models establish that male-female

distance is the strongest predictor of pulse amplitude, and therefore demonstrate that *Drosophila* males perform AMD.

Humans rely primarily on vision for AMD (Zahorik and Kelly, 2007), and the same has been proposed for songbirds (Brumm and Slater, 2006). Do *Drosophila* also utilize vision, a different modality, or multiple cues in combination? We used a panel of genetic and physical manipulations to eliminate individual sensory cues and tested for abnormalities in pulse amplitude modulation. Rendering males deaf or pheromone insensitive, or using females that were unreceptive (Yapici et al., 2008) or lacked pheromones (Billeter et al., 2009) had little effect on the pulse amplitudes produced (Figure 1C, red circles). However, males genetically engineered to be blind (see Experimental Procedures) exhibited a drastically exaggerated mean pulse amplitude compared with their wing length (Figure 1C), with little overlap in the distribution of pulse amplitudes between blind and wild type flies (Figure S3A). Further, we found that AMD is eliminated in blind flies, although only for Dis^{470} > 5mm (Figure 2A, $r^2 = 0.01$; the slopes of black and red points can be compared, but not the absolute values, as they are independently normalized). When comparing absolute (rather than normalized) pulse amplitudes, blind flies sang louder than controls for every value of Dis^{470} (Figure S3B, red and black points are directly comparable in this plot). To confirm that this increase in amplitude was caused by the visual, rather than the genetic, manipulation, we replicated the effect with WT flies by switching lights on/off at regular intervals during courtship (Figure 2B). Blind males showed a normal correlation between male forward velocity and pulse amplitude (Figure S3C), and the relationship between distance and amplitude in blind males was unchanged even after taking this correlation into account (Figure S3D). Together, these results indicate that males use vision to estimate distance and reduce pulse amplitude when close to the female; if completely deprived of visual cues, males default to producing larger pulse amplitudes.

How do males estimate their distance to the female within one body length or < 5mm? We found that the residual AMD observed for blind flies at distances < 5mm was abolished when males were not facing the female (Figure 2C, $r^2 = 0.12$), and that blind males also sang louder pulses when not facing the female (Figure 2D). Thus, AMD within 5mm uses a non-visual sensory cue. When close to the female, males receive olfactory signals from volatile pheromones and perceive non-volatile cuticular pheromones by licking the female or tapping her with their foreleg tarsi (Yamamoto and Koganezawa, 2013). We tested whether these cues could explain residual AMD by examining blind flies with additional sensory deficits. Blind males that were pheromone insensitive, or missing their foreleg tarsi, still produced quieter pulses at close distances, even when females lacked cuticular pheromones (Figure 2E). All blind genotypes failed to modulate amplitude for distances > 5mm ($r^2 \leq 0.25$, Figure S3E). We conclude that another cue from the female (likely a non-gustatory tactile cue) contributes to AMD for close distances. However, even when both facing the female (for |Ang2|<45°) and at close distances, blind flies produced abnormally loud pulses, suggesting that vision is used for AMD at all distances (Figure S3F).

Song amplitude modulation is both fast and dependent on visual history

When modulating a communication signal in real time, the sensorimotor process must be fast enough for the motor output (in this case, the acoustic signal) to have ethological value. However, integrating sensory information over longer time periods can lead to more accurate estimates of sensory information. For AMD in particular, the male fly must accurately estimate female distance but also change his pulse amplitude before the information becomes outdated; in other words, he faces a speed accuracy trade-off when it comes to his reaction time (Chittka et al., 2009). To determine the timescales over which males process visual information to change song behavior, we began by investigating how quickly the male adjusts pulse amplitude with a change in female distance. That is, we asked if males modulate entire song pulse trains based on a single estimation of distance (model 1 or M1), or if the sensorimotor transformation is fast enough for males to modulate individual pulses within each train (model 2 or M2, Figure 3A)? To distinguish between these models, we examined the optimal delay at which Dis is predictive for each pulse position within a train —we expected different results depending on which model is correct (Figure 3B). We separated our data based on pulse number (defined by the position of a pulse within a pulse train (Figure 1A), where each train begins with pulse number one) and built separate GLMs to identify the time point at which distance was most predictive. With the exception of the first two pulses, the most predictive time point was independent of pulse position within a pulse train (Figures 2C and S4A–B). This result supports M2, indicating that males perform AMD on a pulse-by-pulse basis. However, the first two pulses in a train were consistently produced at lower amplitudes (Figure S4C–D), suggesting that there could be a physical limitation during pulse train initiation. If true, pulse numbers one and two should still have a reduced amplitude in the absence of a female. Although males never naturally sing without a female, expression of the heat-sensitive cation channel TrpA1 in specific neural subsets can be utilized to elicit song in isolated males (von Philipsborn et al., 2011). We exploited this thermogenetic strategy to globally activate neurons expressing the sexually dimorphic genes, *fruitless* (FRU^{Act}, ~2000 neurons) and *doublesex* (DSX^{Act}, ~700 neurons). For both genotypes, solitary males (at the activating temperature) produced initial pulses at a reduced amplitude, corroborating the results from wild type data (Figure 3D). We therefore excluded these initial two pulses from all subsequent analyses.

Our GLM results established that distance is optimally predictive ~470ms prior to each pulse (Figure 1F), yet flies rapidly modulate individual pulses (Figure 3C) separated by IPIs of ~35ms (Figure S1D). We thus hypothesized that visual information is integrated over hundreds of milliseconds to improve distance estimation accuracy, but that new information reaches the muscles within a single IPI. This predicts low latency coupling (< 35ms) between changes in the visual stimulus and pulse amplitude. Measuring this latency during natural behavior is not possible because inter-fly distance changes too slowly (Figure S2B). However, we reasoned that a sharp change in ambient light intensity should generate a large burst of neural activity throughout the visual system at a specific time point, and that this visual “shock” would perturb the visual neurons involved in AMD (among many others), producing a change in song amplitude. We toggled the ambient light in our behavioral arena between dark and light conditions, and examined pulse amplitudes from Fru^{Act} males (in the absence of a female). Although such rapid changes in light intensity (see Experimental

Procedures) are unnatural and would not normally be used to estimate distance, FRU^{Act} males produced louder pulses in the dark, an effect not observed in headless FRU^{Act} males (Figure 3E).

To estimate the latency between visual signals and motor output, we generated a rapid and precisely timed perturbation of the visual environment by integrating a voltage controlled light into our behavioral assay and generating an uncorrelated sequence of four ambient light levels between 650lux (moonlit night) and 20,000lux (full daylight). We used this stimulus to probe the time required for visual information to reach the muscles (in other words, to measure the step response of the system). We switched between light levels every 250ms (Video S2). Under these conditions, FRU^{Act} flies increased their pulse amplitude within 30ms of a decrease, but not an increase, in light intensity (Figure 3F). The unidirectional nature of the male's response suggests that visual OFF versus ON pathways are involved in AMD (Behnia et al., 2014). The pulse amplitude changes we observed could not be explained by changes in male velocity (Figure S5A). These results demonstrate, similar to our GLM results above, that signals in the visual pathway influence pulse amplitude within a single IPI, and within ongoing pulse trains. Finally, because males only naturally produce song when in the proximity of and oriented toward the female (Coen et al., 2014), the rapid visual modulation of pulse amplitude we uncovered by stepping the ambient light intensity most likely involves changes in the same visual neurons used to estimate distance to the female.

To test our second prediction—that males integrate visual information over hundreds of milliseconds—we increased the duration at each light level from 250ms to 5s. If visual history beyond 250ms were unimportant, pulse amplitude should be independent of this stimulus duration change. In contrast, we found a 5s period produced much larger, saturated pulse amplitudes for all negative light transitions (Figure 3G–H). We expanded the range of light levels (0.5lux to 20,000lux) and timescales and observed that amplitudes following both 5s and 2s flash periods were saturated, suggesting the period for visual integration lies between 250ms and 2s (Figure S5B). Taken together, these data demonstrate that visual information reaches the muscles within 30ms, but that changes in pulse amplitude depend on visual history extending up to 2s. We hypothesize that this allows the male to accurately estimate distance over a longer timescale while maintaining sensitivity to large, rapid changes in visual stimuli. The use of visual "shock" stimuli uncovered both the latency and effective "memory" of the neural circuit underlying AMD, but to gain an understanding of the neural computations involved, we next determined the specific visual features used to estimate distance to the female.

Dissection of the visual stimulus features used for distance estimation

To dissect the neural circuit computations underlying a sensorimotor transformation, it is critical to determine which features of the sensory stimulus drive changes in the motor output. This is particularly true for AMD because animals can use a variety of visual strategies to estimate distance—some are binocular, such as stereopsis, while others are monocular, such as optical expansion or motion parallax (Stavenga et al., 1989). *Drosophila melanogaster* possess a small region of binocular overlap, comprising the central 30° of their

visual field (Buchner, 1971), and we found that males performed AMD when females occupied either the binocular or monocular region of their visual field ($r^2 \geq 0.92$, Figure 4A). To determine whether monocular vision was sufficient for AMD, we covered the left eye of wild-type males with black paint. These half-blind flies showed a preference for producing song when the female occupied an unblocked region of visual space (Figure 4B). In agreement with our earlier results (Figure 2A), males reduced their pulse amplitude at close distances (< 5mm) for all female locations (Figure S6A), but only modulated their amplitude at larger distances when she was positioned within the visual field of the unblocked eye (Figure 4C). Importantly, even for close distances, half-blind flies sang louder when the female was in the blocked region of visual space, whereas pulses produced by wild-type flies were of a similar amplitude in both visual regions (Figure 4D). Because the different spatial regions provide an internal control (comparing two conditions within each fly), this result cannot be attributed to inter-strain variability and hence demonstrates that—although partly redundant with tactile cues when close to the female—flies utilize monocular vision to modulate amplitude at all distances.

Since males are capable of performing AMD with monocular visual cues, we conclude that the underlying distance estimation circuit does not rely on a comparison between visual signals from the two eyes. Instead, the essential information must be extracted from a single optic lobe. Two principle methods of monocular distance estimation are motion parallax and optical expansion (Bender and Dickinson, 2006; Schuster et al., 2002; Stavenga et al., 1989). These mechanisms rely on the fact that closer objects appear to move across the visual field (motion parallax) or change size (optical expansion) more quickly than distant objects. Thus, female distance could be estimated using the rate of change of her angular location (motion parallax, Δ|Ang2|) or her subtended angle at the male retina (optical expansion, Δ|sAng|); see Figure S2A for an illustration of these angles. However, we found that Dis was a better predictor of pulse amplitude than either Δ|Ang2| or Δ|sAng| (Figure S2A), and male self-motion was not required for AMD ($r^2 = 0.86$, Figure S6B). This suggests that neither optical expansion nor motion parallax, in isolation, can fully explain distance estimation during courtship.

Natural female movement presents a combination of cues to the male. To examine which of these are used to measure distance, we modified the tethered fly-on-the-ball setup utilized in previous studies to investigate visual behaviors (Clark et al., 2011). Tethered flies were induced to sing by thermogenetically activating song command neurons (P1 neurons (Bath et al., 2014; von Philipsborn et al., 2011)) via an infrared laser. We then simultaneously presented visual stimuli at 144Hz and recorded song via two microphones placed directly behind the fly (Figure 4E, Video S3, see Experimental Procedures). Initially, $P1^{Act}$ males were presented with a black square, which smoothly varied in azimuthal location (Ang2 (Figure 1D inset)) and size (Video S4). The stimulus dynamics (Figure 4F) matched the dynamic position of the female (relative to the male) recorded in our behavioral chambers. We define stimulus size as the vertical and horizontal angles (vAng and hAng; Figure 4E) subtended by the square at the fly eye. During natural courtship, vAng changes only with distance (from ~6–14° over distances of 5–12mm, see Experimental Procedures), while hAng changes dramatically depending on female orientation, ranging from ~6° (when the female is 12mm away and her anterior-posterior body axis is in line with the male's) to ~34°

(when 5mm away with perpendicular body axis). We presented a range of stimulus sizes that overlapped with those naturally observed by the male. Because we did not render our image onto a virtual cylinder (Clark et al., 2011), hAng varied with azimuthal position while vAng did not. We presented stimuli in an open-loop regime, so that the effects of visual stimuli on song amplitude could be examined without confounding effects from male motion. Tethered $P1^{Act}$ males performed AMD in response to naturalistic changes in stimulus size and azimuthal location—in other words, they increased pulse song amplitude with decreasing stimulus size ($r^2 \geq 0.83$, Figure 4G). We also recapitulated this result in males in which pIP10 song command neurons (von Philipsborn et al., 2011) were activated instead ($pIP10^{Act}$; $r^2 \geq 0.68$, Figure 4H); pIP10 neurons are downstream of P1 in the song pathway (von Philipsborn et al., 2011) (Figure 6B). These data establish that visual cues are sufficient for driving AMD. They also confirm that males don't use motion parallax to measure distance because the lateral velocity of the stimulus, which corresponds to the speed of the female across the male retina, did not affect amplitude modulation ($r^2 \leq 0.08$, Figure S6C).

We then modified the visual stimulus to test which features were important for AMD. When presented with a stimulus that only changed in size but not in azimuthal position (i.e. it remained at Ang2 = 0, the center of the visual field, Video S5) both genotypes ($P1^{Act}$ and $pIP10^{Act}$) failed to adjust their amplitude in response to stimulus size ($r^2 \leq 0.25$, Figure 4I). We therefore conclude that azimuthal or lateral motion (corresponding to the zig-zagging of the female) is required for AMD. Optical expansion cues (similar to our stimulus) are known to induce escape sequences and flight saccades in standing and airborne flies, respectively, but these behaviors do not require lateral motion (Bender and Dickinson, 2006; Card and Dickinson, 2008). Because escape responses are induced whether the stimulus expands fully or only along a single dimension (i.e. hAng or vAng) (Bender and Dickinson, 2006), we tested the dimensionality dependence of AMD by presenting $P1^{Act}$ and $pIP10^{Act}$ flies with a rectangular stimulus whose vertical and horizontal size varied independently (Video S6). Remarkably, this stimulus did not induce amplitude modulation in either genotype, establishing that AMD requires expansion across two spatial dimensions ($r^2 \leq 0.21$, Figure 4I–J). To our knowledge, this is the first demonstration of a visuomotor behavior in *Drosophila* to exhibit a dependence on correlated changes across two stimulus dimensions (see Discussion for ethological relevance).

Investigating the visual pathways underlying amplitude modulation with distance

The dependence of AMD on lateral motion suggested that the elementary motion detection (EMD) neural pathway could be part of the underlying neural circuit. The EMD pathway is critical for several lateral motion-dependent behaviors in *Drosophila*, including the optomotor response and tracking oscillating vertical bars (Silies et al., 2013). The neural components of the EMD pathway that are required for these behaviors include the lamina output (L1 and L2) and feedback (C2 and C3) neurons, and lobula plate columnar neurons (T4 and T5) (Schnell et al., 2012; Silies et al., 2013; Tuthill et al., 2013) (Figure 5A). In accordance with methods from previous studies(Schnell et al., 2012; Tuthill et al., 2013; Zhu et al., 2009), we silenced these neurons using either the inward rectifying potassium channel Kir2.1 ($L1L2^{Kir}$, $C2C3^{Kir}$, and $T4T5^{Kir}$), Tetanus Toxin Light Chain ($L1L2^{TNT}$, $C2C3^{TNT}$), or temperature-sensitive shibire ($T4T5^{Shi}$), and then tested the role of these neurons in

AMD. For multiple manipulations, we observed defects in the male's ability to follow the female, as illustrated by the increased distance at which males produced song pulses (Figure 5B, D–E). These following defects did not result from decreased mobility (Figure S7A–C). This establishes a previously unidentified role for the EMD pathway in courtship behavior, but despite this following defect, AMD proved robust to all manipulations ($r^2 \geq 0.81$, Figure 5C, F). We used these neural silencing methods to test other neuron classes in the lamina (Tuthill et al., 2013), and also *fruitless*-expressing visual neurons (Yu et al., 2010), but observed no defects in either following behavior or AMD (Figure S7E–J).

The stimulus for the fly-on-the-ball experiments was a looming black square, whose contraction or expansion statistics were drawn from natural behavior (Figure 4)—we therefore tested the role of established loom-sensitive neurons (de Vries and Clandinin, 2012) (termed *Foma1* neurons, Figure 5G) in AMD. We silenced Foma1 neurons ($Foma1^{Shi}$) and, similar to silencing the EMD pathway, observed a significant decrement in male following behavior (Figure 5H), which couldn't be explained by changes in male mobility (Figure S7D). Standing escape is the only behavior previously shown to rely on Foma1 neurons (de Vries and Clandinin, 2012), so a novel role for these neurons in female following during courtship suggests they have a broad, context-dependent function. Despite this, $Foma1^{Shi}$ flies still displayed AMD (Figure 5I, $r^2 = 0.89$; the slopes of black and red points can be compared, but not absolute values, as they are independently normalized), although there may be a minor defect at distances beyond 5mm (beyond 5mm: $r^2 = 0.50$, which is still greater than for blind flies ($r^2 = 0.01$)). We thus conclude that the computations underlying distance estimation are not dependent on identified motion-sensitive and loom-sensitive pathways. This indicates that AMD relies on an as of yet unidentified motion-sensitive visual circuit or stream (see Discussion).

Visual information intersects the song motor pathway in the ventral nerve cord

To map the sensorimotor transformations underlying AMD, it is critical to determine how circuits carrying distance information intersect with the song motor circuit. This circuit starts with command or decision-making neurons in the brain, involves pattern generating neurons, and ultimately connects with motor neurons and muscles that influence the wings (Shirangi et al., 2013; von Philipsborn et al., 2011). We hypothesized two possible circuit mechanisms: either visual signals modulate activity within the neural pathway that controls song (M1), or visual signals directly modulate motor output (M2) (Figure 6A). Four distinct elements of the *Drosophila* song pathway have so far been mapped (von Philipsborn et al., 2011) (Figure 6B). If visual information bypasses this song pathway (M2), artificially activating any of these neurons should not prevent amplitude modulation. Conversely, if visual information intersects with the song pathway (M1), activation below the point of intersection may perturb natural modulation.

We expressed TrpA1 in each of the four neural subsets of the song pathway and confirmed that when placed at an activating temperature (~33°C), all genotypes produced song pulses of normal shape (Figure 6B). We then placed males of all four genotypes with females at the same temperature. Under such conditions, male pulses are elicited through a combination of female cues (when he is facing the female (Figure 1C–E)) and thermogenetic activation.

Indeed, while activated males directed most of their song toward the female, they also produced pulses when not facing her (Figure 6D). Because wild type flies produced < 0.3% of their pulses when not facing the female, we attributed all such pulses to artificial activation. As anticipated from our fly on the ball experiments (Figure 4G–H), both $P1^{Act}$ and $pIP10^{Act}$ males performed AMD in response to visual cues from the female ($r^2 \geq 0.76$, Figure 6E, G). When not facing the female, these males produced pulses at a constant amplitude, and these artificial pulses were louder than those directed toward the female (Figure 6F, H). In agreement with our results from visually deprived flies (Figure S3B), this result suggests that flies default to high pulse amplitudes when they do not receive visual cues. In contrast, $dPR1^{Act}$ males showed a reversal of the natural behavior, increasing pulse amplitude when closer to or facing the female ($r^2 = 0.52$, Figure 6I–J) and $vPR6^{Act}$ flies sang at constant amplitude irrespective of female location ($r^2 \leq 0.16$, Figure 6K–L). This demonstrates that visual information intersects with the song pathway (M1, Figure 6A), and suggests that this intersection occurs downstream of the pIP10 but upstream of the dPR1 neuron. vPR6 neurons are putative central pattern generating (CPG) neurons, as constitutive activation of these neurons has been shown to alter the rate at which pulses are produced, or the IPI. However, we found no correlation between IPI and pulse amplitude during courtship (Figure S1E–F), suggesting that a single song circuit independently regulates pulse timing and amplitude (see Discussion).

Song amplitude modulation involves the indirect flight muscles

After intersecting with the song pathway, visual information must eventually influence muscle activity to change song amplitude. During flight, two primary muscle groups control wing movement in *Drosophila*: the direct flight muscles, which attach to the base of the wing (Ewing, 1979), and the indirect flight muscles (IFMs), which attach to the thorax (Ewing, 1977). Both muscle-types are active during song (Ewing, 1979, 1977), but a recent study suggested that the IFMs do not significantly contribute to song production (Chakravorty et al., 2014). As the IFMs are required to generate power during flight (Moore et al., 2000), we hypothesized that they were also required for AMD. Dual, a double mutation of the *Drosophila* myosin regulatory light chain (Dmlc2), is known to cause defects in the contractile properties of IFMs, and has therefore been used to examine the role of these muscles in both flight and song (Chakravorty et al., 2014; Farman et al., 2009). Compared with controls, Dual mutant flies produced pulses at an abnormally low amplitude given their wing length (Figure 6M), and also generated lower pulse amplitude variability (Figure S8C). However, these flies still produce normal pulse shape (Figure S8A), albeit exhibiting a decrease in pulse fundamental frequency expected from quieter pulses (Figure S8B, and S1G–K). Strikingly, Dual mutant flies exhibited a near complete lack of amplitude modulation with either increasing Dis^{470} or mFV^{100} (Figure 6N, and S8B). This suggests a critical role for these muscles in AMD, and in other forms of sensorimotor pulse amplitude modulation.

Dmlc2 mutations are known to affect the IFMs, but from these genetic experiments alone, we cannot exclude the possibility that the observed loss of AMD results from a defect in another muscle group. However, if the IFMs are responsible for AMD, IFM spiking activity should correlate with pulse amplitude. Unlike the direct flight muscles, the 13 IFMs (Ewing,

1977) fire tonically with an inter-spike-interval roughly double the IPI (Ewing, 1979). We hypothesized that changes in pulse amplitude should be reflected in the IFM firing rate. To test this, we performed extracellular recordings from individual IFMs while simultaneously measuring the amplitude of song pulses produced by $P1^{Act}$ flies heated with a laser (see Experimental Procedures). Consistent with previous reports (Ewing, 1979), we also did not observe precise phase-locking between spiking of individual IFMs and song pulses (Figure 6O, inset). Nonetheless, we observed a strong correlation between spike rate and pulse amplitude ($r^2 = 0.81$, Figure 6O), but no correlation with IPI ($r^2 = 0.02$, Figure 6O). Together with our genetic manipulations, this suggests that control of pulse amplitude is achieved through modulation of IFM drive. Because the direct flight muscles have been implicated in controlling the temporal structure of song (Ewing, 1979, 1977; Shirangi et al., 2013), our data provide a mechanism by which the fly can adjust song amplitude (via the IFMs) without altering the temporal pattern.

Discussion

The ability to modulate acoustic signal amplitude with distance to a communication partner (what we refer to in this study as **AMD**) had previously only been demonstrated in humans and songbirds (Brumm and Slater, 2006; Zahorik and Kelly, 2007). Here, we have not only established that *Drosophila melanogaster* males also perform AMD, utilizing visual cues to estimate receiver distance and modulate the intensity of their acoustic communication signals accordingly, but have also probed each stage of the sensorimotor transformation underlying this behavior, via a combination of quantitative assays, statistical modeling of a large behavioral dataset, genetic and neural circuit manipulations, and electrophysiology. Our investigation extended from the dynamics of the visual stimulus through the nervous system to the eventual modulation of muscle activity (Figure 7).

The Relevance of AMD

AMD was previously thought to rely on cognitive abilities (Johnson et al., 1981)—in other words, the capacity to take the perspective of the listener and to make compensations that serve his or her needs. The demonstration of AMD in *Drosophila* suggests, in contrast, that this innate ability also exists to serve the needs of the singer or speaker. *Drosophila* males, in contrast with humans and songbirds, are limited to communicating over relatively short distances. This arises in part from the small size of their wings—each wing maximally generates only ~10^{-16} W of power, which is roughly six orders of magnitude below the threshold of human hearing (Bennet-Clark, 1971). In addition, the *Drosophila* ear (its arista) is most sensitive to the particle velocity component of sound, which is heavily attenuated with increasing distance from a point source (Göpfert and Robert, 2002; Morley et al., 2012). To increase the probability that the female hears his song, the male could continually sing at maximal intensity, but this runs the risk of saturating her auditory system and consequently making his communication signal less effective. By dynamically adjusting his song intensity to compensate for changes in her distance as he chases her, the male not only keeps his song within the dynamic range of her auditory receiver (Nadrowski et al., 2010), but also likely conserves his own energy. Since *Drosophila* males often court females for upwards of 10 minutes and sing thousands of pulses before copulating (Coen et al., 2014)

performing AMD is likely to be energy efficient (although the energetic cost of fly song has yet to be quantified).

The Timescales of AMD

When estimating female distance from sensory cues, *Drosophila melanogaster* males must balance the need to adjust song amplitude before their distance to the female changes with the benefit of integrating more information to better estimate that distance; that is, AMD is subject to a speed accuracy trade-off, similar to many decision-making behaviors (Chittka et al., 2009). To identify the timescales underlying AMD, we used a novel experimental strategy to "shock" the visual system with rapid changes of light intensity during thermogenetic activation of singing. Although such visual stimuli are unnatural, they elicited transient changes in pulse amplitude within 30ms, indicating that the visual neurons involved in AMD were among those responding to the visual "shock." This rapid timescale is closely matched to the *Drosophila melanogaster* inter-pulse interval or IPI (~35ms), raising the possibility that the visual pathway used to estimate distance to the female is optimized for the modulation of individual pulses. Although it is possible that the visual neurons causing an amplitude response to light flashes are not those involved in natural AMD, we think this improbable because i) amplitude changes were dependent on historical timescales (250ms-2s) similar to those predicted from a GLM based on natural behavior (470ms), and ii) it is unlikely that two separate visual pathways both modulate pulse song amplitude. Moreover, the integration timescale we suggest (250ms-2s) agrees with prior work on distance estimation, which found that *Drosophila* could identify the closer of two stationary objects even if visual feedback was delayed by 2s (Schuster et al., 2002). The duality between visual integration time (250ms-2s) and response latency (30ms) is particularly interesting as there are a scarcity of identified behaviors in *Drosophila* that involve integration of sensory information over longer timescales, with the exception of angular path integration (Seelig and Jayaraman, 2015). Thus, AMD presents a novel opportunity to study the dynamic integration of visual information.

Visual Stimulus Features and Visual Pathways

Flies are known to assess their distance from stationary objects using visual cues (Cabrera and Theobald, 2013; Schuster et al., 2002), but distance estimation in the context of a translating and rotating object (the female during courtship) is a special case. We found that it shows a unique dependence on correlated changes in visual stimulus size across two dimensions. This makes sense because female rotation causes uneven changes in her vertical and horizontal subtended angles at the male eye (vAng and hAng), while changes in distance will cause these two angles to vary in unison. Thus, we postulate that the two-dimensional stimulus dependence of AMD allows males to maintain a rotation-invariant response to female distance and avoid unwanted changes in pulse amplitude. We then tested the involvement of identified visual pathways in processing these unique visual stimulus features. Our neural silencing experiments demonstrated a novel role for the identified elementary motion-sensitive and loom motion-sensitive pathways in following the female during courtship. However, our data do not support a role for these pathways in AMD. This suggests that distinct neural pathways underlie tracking the female versus estimating her distance. Although we have not yet identified the specific neurons responsible for AMD, the

visual computations we found to underlie distance estimation resemble those of the small target motion detectors studied in other insects (Nordström, 2012). These neurons are located in the lobula and are identified by their sharp size tuning: they respond to targets subtending 1–3 degrees of the visual field, with no response to wide-field gratings or bars (Nordström, 2012). They are also thought to act in a parallel pathway to the EMD pathway, yet are still sensitive to lateral motion. Further, their response profile has been shown to shift with changes in object size—a larger object will need to move at greater lateral speed to elicit the same response (Geurten et al., 2007). Although small target motion detectors have yet to be identified in *Drosophila*, recent work has identified a group of lobula plate neurons that encode the features required for a separate but similar behavior known as figure detection (Aptekar et al., 2015)—identifying a foreground stimulus moving against a distinct background. It is possible that these neurons have an important role in AMD, but as they were not probed with small visual targets, their potential role is still unclear.

Modulation of Activity in the Song Motor Pathway

The *Drosophila* song pathway begins with a subset of ~20 neurons in the *doublesex*-expressing pC1 neural cluster of the protocerebrum in the brain (von Philipsborn et al., 2011, Kimura et al., 2008). These neurons receive information from courtship-relevant sensory pathways (e.g., those that carry pheromonal (Clowney et al., 2015; Kohatsu et al., 2010), visual (Kohatsu and Yamamoto, 2015) and auditory (Zhou et al., 2015) cues) and synapse onto motor “command neurons” (e.g. pIP10 (von Philipsborn et al., 2011)). Thus, P1 neurons are thought to lie at the sensory-motor interface within the *Drosophila* brain. In contrast, we have now shown that neurons that carry visual information (in particular, information about distance to the female) intersect with the song motor pathway downstream of P1, and even pIP10, in the ventral nerve cord (VNC). This result has implications for the notion of “command neurons”; in this case, the motor pattern produced by the fly remains undetermined until later in the neural pathway, with neurons in the VNC that receive sensory input playing an instructive role in song patterning.

Prior studies of central pattern generator (CPG) function have shown that increased drive to the CPG changes both the intensity and timing of behaviors such as stepping and swimming (Gabriel and Büschges, 2007; Sirota et al., 2000). Conversely, ideal AMD requires an animal to change acoustic intensity without affecting the timing or rate of the acoustic signal (in other words, singing louder should not necessarily mean singing faster). We have shown that visual information intersects with the song pathway upstream of neurons that control song pulse timing (vPR6) (von Philipsborn et al., 2011), and that pulse amplitude changes occur independent of inter-pulse interval changes (see Figure S1). Our genetic manipulations and extracellular recordings suggest that visual signals eventually impact activity in the indirect flight muscles (IFMs). Neural recordings have previously shown that direct flight muscles spike in time with each song pulse whereas IFMs show tonic activity with an inter-spike interval approximately double that of the IPI (Ewing, 1979). Taken together, these results suggest a dual output of the song CPG, controlling pulse rate and amplitude via the direct and indirect flight muscles, respectively (Figure 7). Just as the spectral and temporal aspects of acoustic signals seem to be independently controlled in many systems, including songbirds (Ali et al., 2013) and humans (Cai et al., 2011), our results suggest that intensity is

also independently regulated. How this occurs in *Drosophila* within a single circuit remains to be solved. Finally, our findings add to the growing evidence that variability in natural behavior represents ethologically advantageous responses to sensory stimuli (Calhoun et al., 2014; Censi et al., 2013; Coen et al., 2014; Mischiati et al., 2015). In other words, fluctuations in *Drosophila* courtship song amplitude are not a result of neural noise, but rather a carefully orchestrated process to match male song intensity to female position. *Drosophila* AMD may represent an example of convergent evolution, given that birds, humans and flies shared a common ancestor >800 million years ago. Nonetheless, solving the sensorimotor transformations underlying the modulation of song intensity with communication distance in flies promises to shed light on the computations and mechanisms that form the building blocks for social interactions across the animal kingdom.

Experimental Procedures Summary

Fly strains and rearing

Fly stocks and genotypes are detailed in Supplemental Experimental Procedures.

Behavior

Behavioral experiments (simultaneous song and fly movement recordings) on untethered flies were carried out as described previously (Coen et al., 2014). To change the light intensity in the chamber, a 3″ white LED ring light (Edmund Optics) was adjusted using an analog voltage signal. For tethered fly-on-the-ball experiments, designs for the ball holder were provided by Vivek Jayaraman (Seelig et al., 2011) and flies were tethered using a protocol provided by Michael Reiser (Reiser and Dickinson, 2008). Stimuli were delivered with a single XL2411T monitor (BenQ) at 144Hz using Psychtoolbox-3 (MATLAB, Mathworks). An 808nm laser (Dragon Lasers) was used to heat flies. Visual stimuli were generated using tracking statistics from freely moving $P1^{Act}$ males paired with PIBL females, and then these stimuli were manipulated in subsequent experiments. See Supplemental Experimental Procedures for further details and modifications of the tethered fly preparation for simultaneous electrophysiology.

Neural activation and silencing

Visual neurons were inactivated in accordance with prior studies (Schnell et al., 2012; et al., 2013; de Vries and Clandinin, 2012). Song-pathway neurons were activated using TrpA1 (von Philipsborn et al., 2011) and the environment was heated to the activating temperature before placing flies in the behavioral chamber. See Supplemental Experimental Procedures further details.

Data processing

All data processing and analyses were conducted in MATLAB (MathWorks, Inc.). For each fly, pulse amplitudes were normalized for fly position relative the microphone and z-scored. Thus, pulse amplitudes are reported in standard deviations from the mean. Fly tracking and song segmentation were performed as previously described (Coen et al., 2014; Deng et al., 2013). For further details and quantification of song and movement features, see Supplemental Experimental Procedures.

Data analyses

The GLM implementation was modified from prior work (Coen et al., 2014) to account for analog output data (amplitudes). To test for amplitude modulation, normalized amplitude was binned by inter-fly distance and r^2 values were calculated for linear fits. The same methodology was applied for fly-on-the-ball and electrophysiological analyses, with distance replaced by stimulus size or spike rate respectively. To test for an amplitude response to a change in light intensity, pulse amplitudes pre- and post-intensity change were compared. Detailed explanations of analyses are included in Supplemental Experimental Procedures.

Supplementary Material

Refer to Web version on PubMed Central for supplementary material.

Acknowledgments

We thank Thomas Clandinin, Dmitriy Aronov, Adam Calhoun, David Deutsch, Matteo Carandini, and Kenneth Harris for comments on the manuscript. We thank Xiao-Juan Guan for technical assistance and Andrew Weinstein, who contributed to preliminary experiments. PC was funded by an HHMI International Pre-Doctoral Fellowship, JC was funded by the DAAD (German Academic Exchange Foundation), and MM is funded by the Alfred P. Sloan Foundation, Human Frontiers Science Program, National Science Foundation CAREER award, NIH New Innovator Award, NSF BRAIN Initiative EAGER award, McKnight Foundation, and Klingenstein-Simons Foundation.

References Cited

Alexander R. Aggressiveness, Territoriality, and Sexual Behavior in Field Crickets (Orthoptera: Gryllidae). Behaviour. 1961; 17:130–223.

Ali F, Otchy T, Pehlevan C, Fantana A, Burak Y, Ölveczky B. The Basal Ganglia Is Necessary for Learning Spectral, but Not Temporal, Features of Birdsong. Neuron. 2013; 80

Aptekar, Kele; Lu, Zolotova; Frye. Neurons Forming Optic Glomeruli Compute Figure-Ground Discriminations in Drosophila. Journal of Neuroscience. 2015; 35:75877599.

Bath D, Stowers J, Hörmann D, Poehlmann A, Dickson B, Straw A. FlyMAD: rapid thermogenetic control of neuronal activity in freely walking Drosophila. Nature Methods. 2014; 11

Behnia R, Clark D, Carter A, Clandinin T, Desplan C. Processing properties of ON and OFF pathways for Drosophila motion detection. Nature. 2014; 512:427–430. [PubMed: 25043016]

Bender J, Dickinson M. Visual stimulation of saccades in magnetically tethered Drosophila. The Journal of experimental biology. 2006; 209:3170–82. [PubMed: 16888065]

Bennet-Clark HC. Acoustics of insect song. Nature. 1971; 234:255–259.

Billeter JC, Atallah J, Krupp J, Millar J, Levine J. Specialized cells tag sexual and species identity in Drosophila melanogaster. Nature. 2009; 461:987–91. [PubMed: 19829381]

Brumm H, Slater P. Animals can vary signal amplitude with receiver distance: evidence from zebra finch song. Animal Behaviour. 2006; 72:699705.

Buchner, E. Dunkelanregung des stationaren Flugs der Fruchtfliege Drosophila. Univ Tiibingen; 1971.

Cabrera S, Theobald J. Flying fruit flies correct for visual sideslip depending on relative speed of forward optic flow. Frontiers in Behavioral Neuroscience. 2013; 7

Cai S, Ghosh S, Guenther F, Perkell J. Focal Manipulations of Formant Trajectories Reveal a Role of Auditory Feedback in the Online Control of Both Within-Syllable and Between-Syllable Speech Timing. The Journal of Neuroscience. 2011; 31

Calhoun A, Chalasani S, Sharpee T. Maximally informative foraging by Caenorhabditis elegans. eLife. 2014; 3

Card G, Dickinson M. Visually Mediated Motor Planning in the Escape Response of Drosophila. Current Biology. 2008; 18

Censi A, Straw A, Sayaman R, Murray R, Dickinson M. Discriminating External and Internal Causes for Heading Changes in Freely Flying Drosophila. PLoS Computational Biology. 2013; 9

Chakravorty S, Vu H, Foelber V, Vigoreaux J. Mutations of the Drosophila Myosin Regulatory Light Chain Affect Courtship Song and Reduce Reproductive Success. PLoS ONE. 2014; 9

Chittka L, Skorupski P, Raine NE. Speed–accuracy tradeoffs in animal decision making. Trends in Ecology & Evolution. 2009; 24:400–407. [PubMed: 19409649]

Clark D, Bursztyn L, Horowitz M, Schnitzer M, Clandinin T. Defining the computational structure of the motion detector in Drosophila. Neuron. 2011; 70:1165–77. [PubMed: 21689602]

Clowney, Iguchi S, Bussell J, Scheer E, Ruta V. Multimodal Chemosensory Circuits Controlling Male Courtship in Drosophila. Neuron. 2015; 87:1036–49. [PubMed: 26279475]

Coen P, Clemens J, Weinstein A, Pacheco D, Deng Y, Murthy M. Dynamic sensory cues shape song structure in Drosophila. Nature. 2014; 507:233–7. [PubMed: 24598544]

Deng Y, Coen P, Sun M, Shaevitz J. Efficient multiple object tracking using mutually repulsive active membranes. PloS one. 2013; 8:e65769. [PubMed: 23799046]

Ewing A. The neuromuscular basis of courtship song in Drosophila: The role of the indirect flight muscles. Journal of comparative physiology. 1977; 119:249–265.

Ewing A. The neuromuscular basis of courtship song in Drosophila: The role of the direct and axillary wing muscles. Journal of comparative physiology. 1979; 130:87–93.

Farman G, Miller M, Reedy M, Soto-Adames F, Vigoreaux J, Maughan D, Irving T. Phosphorylation and the N-terminal extension of the regulatory light chain help orient and align the myosin heads in Drosophila flight muscle. Journal of structural biology. 2009; 168:240–9. [PubMed: 19635572]

Gabriel J, Büschges A. Control of stepping velocity in a single insect leg during walking. Philosophical Transactions of the Royal Society A: Mathematical, Physical and Engineering Sciences. 2007; 365:251–271.

Geurten B, Nordström K, Sprayberry J, Bolzon D, O'Carroll D. Neural mechanisms underlying target detection in a dragonfly centrifugal neuron. Journal of Experimental Biology. 2007; 210:3277–3284. [PubMed: 17766305]

Göpfert MC, Robert D. The mechanical basis of Drosophila audition. Journal of Experimental Biology. 2002

Johnson C, Pick H, Siegel G, Cicciarelli A, Garber S. Effects of Interpersonal Distance on Children's Vocal Intensity. Child Dev. 1981; 52

Kimura KI, Hachiya T, Koganezawa M, Tazawa T, Yamamoto D. Fruitless and doublesex coordinate to generate male-specific neurons that can initiate courtship. Neuron. 2008; 59:759–69. [PubMed: 18786359]

Kohatsu S, Koganezawa M, Yamamoto D. Female Contact Activates Male-Specific Interneurons that Trigger Stereotypic Courtship Behavior in Drosophila. Neuron. 2010; 69

Kohatsu S, Yamamoto D. Visually induced initiation of Drosophila innate courtship-like following pursuit is mediated by central excitatory state. Nat Commun. 2015; 6:6457. [PubMed: 25743851]

Mineault P, Barthelmé S, Pack C. Improved classification images with sparse priors in a smooth basis. Journal of Vision. 2009; 9

Mischiati M, Lin HT, Herold P, Imler E, Olberg R, Leonardo A. Internal models direct dragonfly interception steering. Nature. 2015; 517:333–338. [PubMed: 25487153]

Moore J, Dickinson M, Vigoreaux J, Maughan D. The Effect of Removing the N-Terminal Extension of the Drosophila Myosin Regulatory Light Chain upon Flight Ability and the Contractile Dynamics of Indirect Flight Muscle. Biophysical Journal. 2000; 78:1431–40. [PubMed: 10692328]

Morley EL, Steinmann T, Casas J, Robert D. Directional cues in Drosophila melanogaster audition: structure of acoustic flow and inter-antennal velocity differences. The Journal of experimental biology. 2012; 215:2405–2413. [PubMed: 22723479]

Nadrowski B, Effertz T, Senthilan P, Göpfert M. Antennal hearing in insects – New findings, new questions. Hearing Research. 2010; 273

Nordström K. Neural specializations for small target detection in insects. Current Opinion in Neurobiology. 2012; 22

Philipsborn A, von Liu T, Yu J, Masser C, Bidaye S, Dickson B. Neuronal Control of Drosophila Courtship Song. Neuron. 2011; 69

Reiser M, Dickinson M. A modular display system for insect behavioral neuroscience. Journal of Neuroscience Methods. 2008; 167

Schnell B, Raghu S, Nern A, Borst A. Columnar cells necessary for motion responses of wide-field visual interneurons in Drosophila. Journal of Comparative Physiology A. 2012; 198:389–395.

Schuster S, Strauss R, Götz K. Virtual-reality techniques resolve the visual cues used by fruit flies to evaluate object distances. Current biology : CB. 2002; 12:1591–4. [PubMed: 12372251]

Seelig J, Chiappe E, Lott G, Dutta A, Osborne J, Reiser M, Jayaraman V. Two-photon calcium imaging from head-fixed Drosophila during optomotor walking behavior. Nature Methods. 2011; 7

Seelig J, Jayaraman V. Neural dynamics for landmark orientation and angular path integration. Nature. 2015; 521

Shirangi T, Stern D, Truman J. Motor Control of Drosophila Courtship Song. Cell Reports. 2013; 5:678–86. [PubMed: 24183665]

Silies M, Gohl D, Clandinin T. Motion-detecting circuits in flies: coming into view. Annual review of neuroscience. 2013; 37:307–27.

Sirota, Prisco D, Dubuc. Stimulation of the mesencephalic locomotor region elicits controlled swimming in semi-intact lampreys. The European journal of neuroscience. 2000; 12:4081–92. [PubMed: 11069605]

Stavenga D, Hardie R, Schwind R. Size and Distance Perception in Compound Eyes. Facets of Vision. 1989

Tauber, Eberl. Song production in auditory mutants of Drosophila: the role of sensory feedback. Journal of comparative physiology A, Sensory, neural, and behavioral physiology. 2001; 187:341–8.

Tuthill J, Nern A, Holtz S, Rubin G, Reiser M. Contributions of the 12 neuron classes in the fly lamina to motion vision. Neuron. 2013; 79:128–40. [PubMed: 23849200]

de Vries S, Clandinin T. Loom-sensitive neurons link computation to action in the Drosophila visual system. Current biology : CB. 2012; 22:353–62. [PubMed: 22305754]

Yamamoto D, Koganezawa M. Genes and circuits of courtship behaviour in Drosophila males. Nature reviews Neuroscience. 2013; 14:681–92. [PubMed: 24052176]

Yapici N, Kim YJ, Ribeiro C, Dickson B. A receptor that mediates the post-mating switch in Drosophila reproductive behaviour. Nature. 2008; 451:33–7. [PubMed: 18066048]

Yu J, Kanai M, Demir E, Jefferis G, Dickson B. Cellular Organization of the Neural Circuit that Drives Drosophila Courtship Behavior. Current Biology. 2010; 20:1602–14. [PubMed: 20832315]

Zahorik P, Kelly J. Accurate vocal compensation for sound intensity loss with increasing distance in natural environments. The Journal of the Acoustical Society of America. 2007; 122:EL143–EL150. [PubMed: 18189448]

Zhou C, Franconville R, Vaughan A, Robinett C, Jayaraman V, Baker B. Central neural circuitry mediating courtship song perception in male Drosophila. eLife. 2015; 4

Zhu Y, Nern A, Zipursky L, Frye M. Peripheral Visual Circuits Functionally Segregate Motion and Phototaxis Behaviors in the Fly. Current Biology. 2009; 19

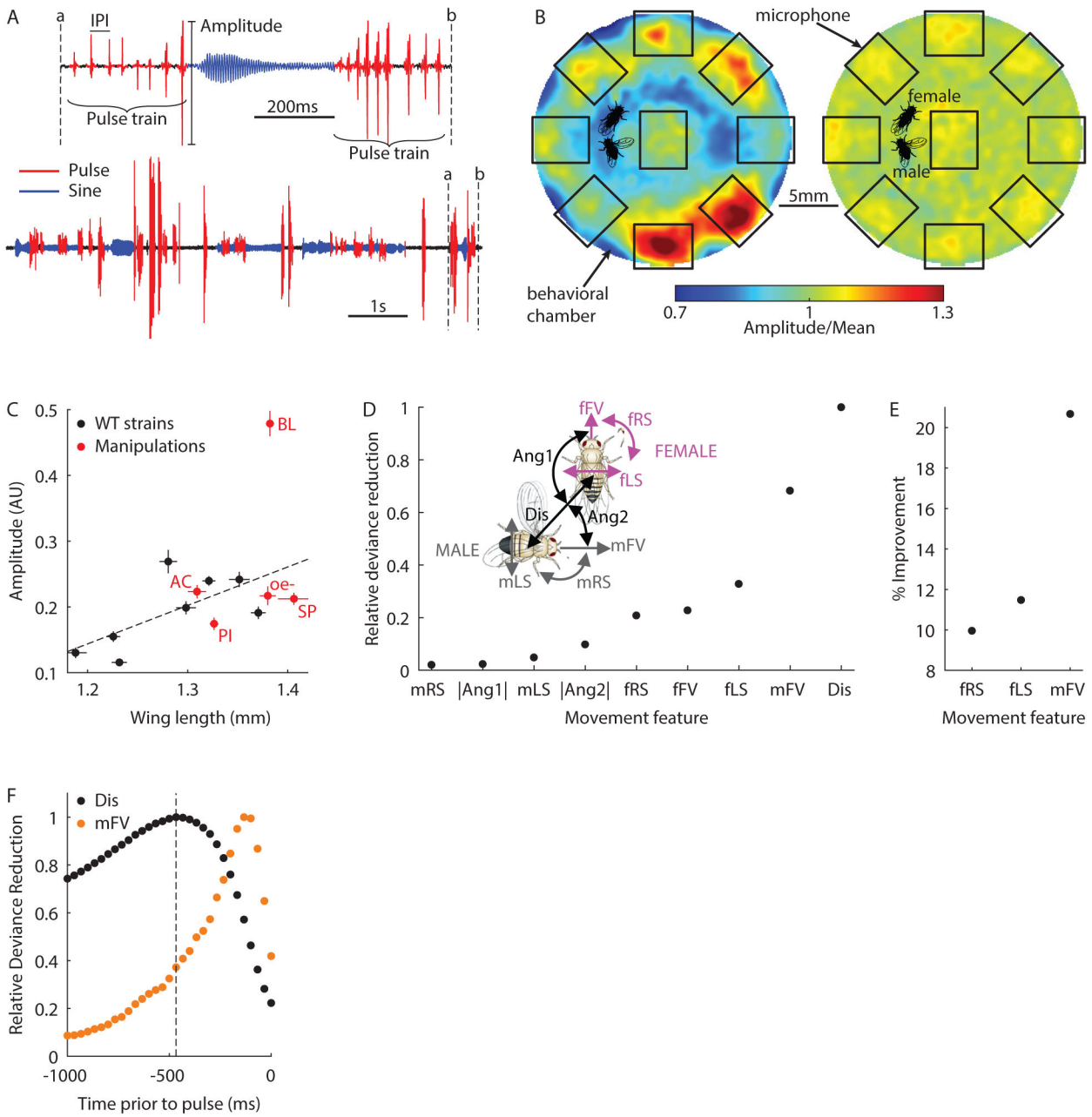

Figure 1. Song amplitude modulation with distance in *Drosophila*

A, *Drosophila* song is composed of pulse (red) and sine (blue) elements. Males produce trains of pulses which vary in amplitude and are separated by species-typical inter-pulse intervals (IPI). **B**, Pulse amplitudes for each male position within the chamber (as a fraction of the overall mean amplitude) before (left) and after (right) normalization (n = 795,152 pulses from 380 flies, see Experimental Procedures). Microphone positions and fly images are included for scale. **C**, Mean pulse amplitude (arbitrary units) versus wing length across 8 wild type strains (black, n = 28–39 flies). Five manipulations are also shown (red, n = 11–30 flies): deaf (AC for arista cut), blind (BL), or pheromone insensitive (PI) males paired with pheromone insensitive and blind (PIBL) females, and WT1 males paired with unreceptive

females (SP for sex peptide injected) or females genetically engineered to lack pheromone producing cells (oe-). Linear fit (dashed line) is for wild type data only ($r^2 = 0.46$). All flies included in this plot sang > 200 pulses. Error bars indicate SEM. **D**, Relative deviance reduction for generalized linear models (GLMs) designed to predict amplitude from a single feature (see Experimental Procedures). **Inset**, Illustration of 9 features used as predictors in the GLM: male/female forward velocity (mFV/fFV), male/female lateral and rotational speeds (mLS/fLS and mRS/fRS), the distance between fly centers (Dis), the absolute angle from female/male heading to male/female center (Ang1/Ang2). **E**, The percentage improvement in the model after combining Dis with a second feature. **F**, Relative deviance reduction for GLMs designed to predict amplitude from Dis (black) or mFV (orange) at specified delays prior to each pulse. Dashed line highlights maximally predictive time point for Dis (−470ms). **D–F**, n = 361,817 pulses from 226 flies, 95% confidence intervals are too small to visualize. Each fly sang > 500 pulses. (See also Figures S1 and S2)

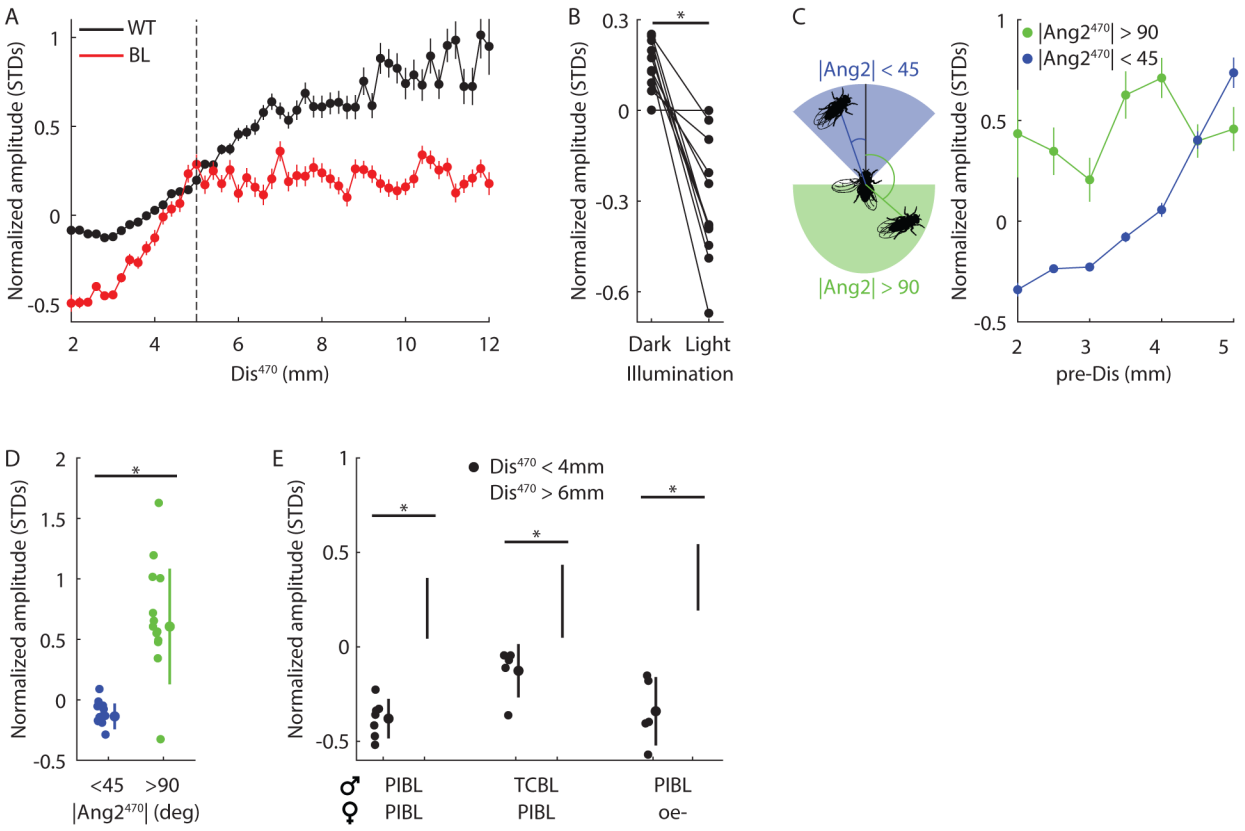

Figure 2. The role of vision in AMD

A, Normalized amplitude (measured in standard deviations (STDS) from the mean) versus distance at 470ms prior to the pulse (Dis^{470}). Bin width 0.2mm for all WT (black, n = 226 flies) and BL (red, n = 25 flies) males. Dashed line indicates 5mm boundary, beyond which BL flies did not exhibit amplitude modulation with distance (AMD). For Dis^{470} below and above 5mm, $r^2 = 0.85/0.94$, and $r^2 = 0.80/0.01$ for WT/BL flies. > 100 pulses contributed to each point. **B**, WT1 males (paired with PIBL females) produced louder pulses in the dark. *$P < 10^{-4}$, n = 12 flies singing > 200 pulses in each condition. Lights were switched on or off every 15s during courtship. **C**, **Left**, Illustration of regions within the male visual field that constitute |Ang2| < 45° (blue) or |Ang2| > 90° (green). **Right**, For pulses produced by BL flies at Dis^{470} < 5mm (bin width 0.5mm), amplitude was dependent or independent of Dis^{470} if the male faced toward ($|Ang2|^{470}$ < 45°, blue, $r^2 = 0.94$) or away from ($|Ang2|^{470}$ > 90°, green, $r^2 = 0.12$) the female. > 25 pulses contributed to each point. n = 25 flies. **D**, Blind flies sang louder pulses at Dis^{470} < 4mm (chosen to avoid 5mm boundary) when facing the female (blue) versus when facing away from her (green). *$P < 10^{-5}$, n = 13 flies singing > 10 pulses in each condition. **E**, PIBL or TCBL (tarsi cut and blind) males reduced amplitude when close to the female (Dis^{470} < 4mm, closed circles), even when paired with oe-females (PIBL males only). *P < 0.05, n = 5–7 flies singing > 100 pulses in each condition. **A–D** Each fly sang > 500 pulses. **A** and **C,** error bars indicate SEM. **D–E**, individual flies, mean, and STD are shown. (See also Figures S1, S2 and S3)

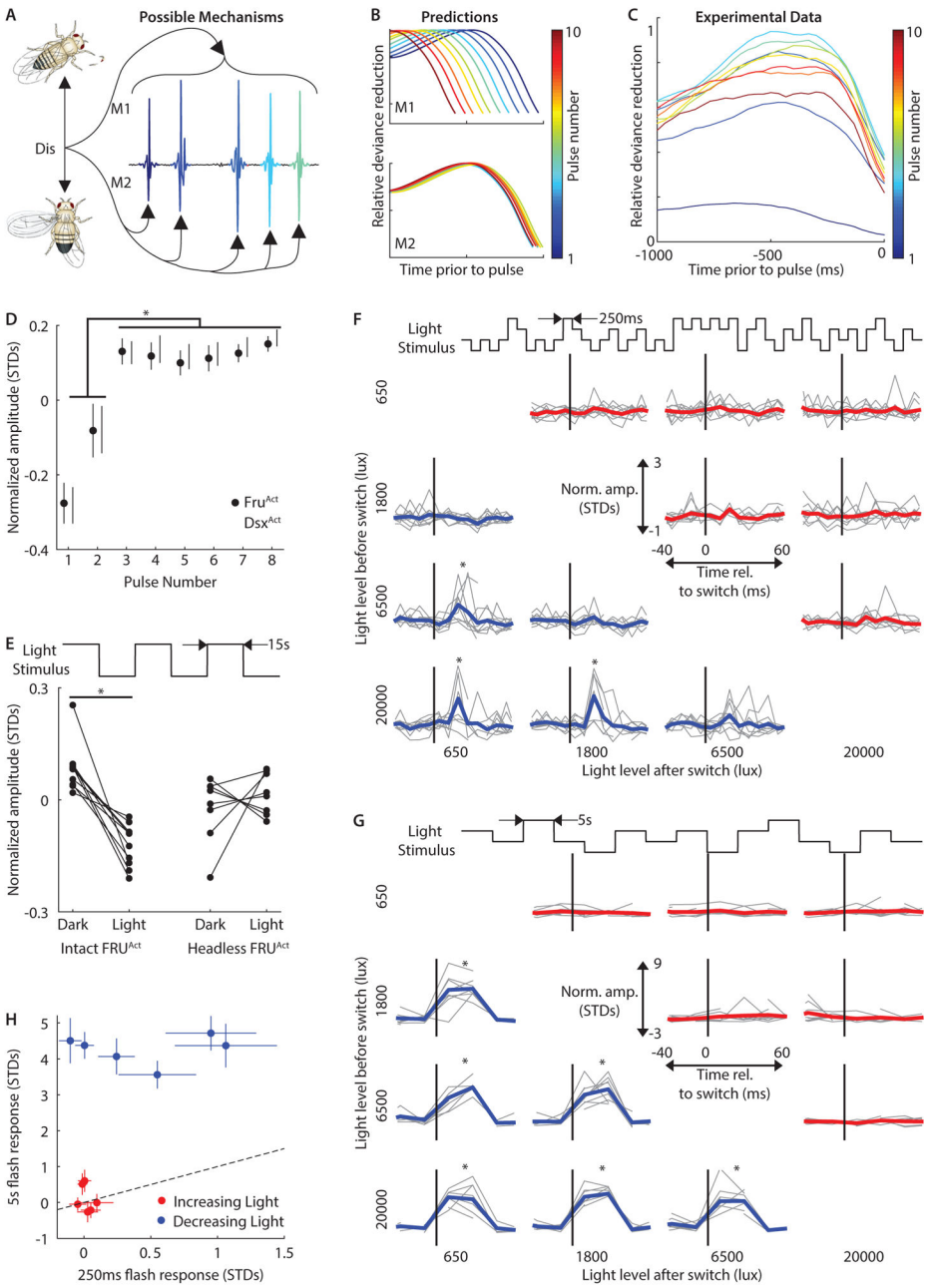

Figure 3. Timescales of AMD

A, Possible mechanisms for amplitude modulation with distance (AMD). Either distance information modulates entire pulse trains (top, M1) or each individual pulse (bottom, M2). **B**, Predictions for relative deviance reduction from GLMs (compare with Fig. 1F) for the two mechanisms in **A** if data were separated by pulse number and GLMs were designed to predict amplitude from the Dis feature at the specified delays prior to each pulse. **C**, Relative deviance reduction curves from the data support M2. n = 15,648–52,478 pulses from 226 flies for each GLM. **D**, Normalized amplitude for each pulse number produced by FRU^{Act} (activated *fruitless*-expressing neurons, closed circles) and DSX^{Act} (activated *doublesex*-

expressing neurons, open circles) males without a female. *P < 0.05, n = 4–9 flies singing > 100 pulses for each point. Genotypes were combined for ANOVA. **E**, When switching between light conditions every 15s (see Experimental Procedures), FRU^{Act} flies sang louder pulses in the dark (n = 10, *P < 0.001) but not if headless (n = 8, P > 0.4). Each fly sang > 200 pulses during each condition (light or dark). **F**, Light-transition-triggered average for normalized amplitude produced by FRU^{Act} flies relative to increases (red) or decreases (blue) in light intensity. Intensity switches (between 4 light levels) occurred every 250ms (bin width 10ms, black line = 0ms). Data from Individual flies are in gray. *P < 0.05, n = 5–9 flies in each time bin. **G**, As in **F**, but for switches every 5s (bin width 25ms). * P < 0.01, n = 3–10 flies in each time bin. **H**, Pulse amplitude response (defined in Experimental Procedures) for 250ms versus 5s stimuli (see Experimental Procedures). Pulse amplitudes following decreasing light switches (blue) but not increasing light switches (red) were larger for 5s stimuli (blue, P < 0.01; red, P > 0.08). n = 5–10 flies. **E** and **H**, Error bars indicate SEM. **C–G** Each fly sang > 500 pulses. (See also Figures S4 and S5)

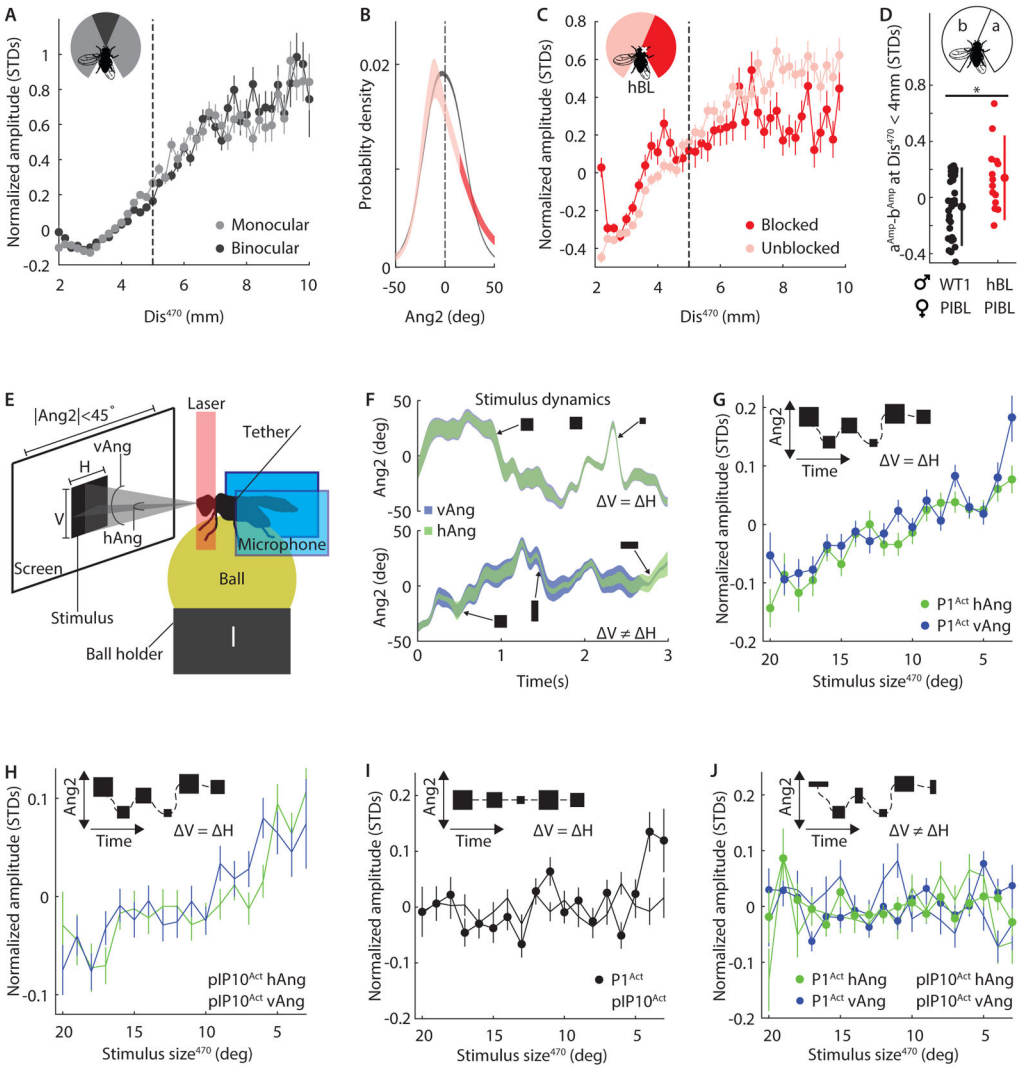

Figure 4. Computations underlying distance estimation

A, Normalized amplitude versus Dis^{470} (bin width 0.2mm) for all WT males. Data was split into times when the female occupied the binocular (dark gray, $|Ang2|^{470} < 15°$, $r^2 = 0.94$) or monocular (light gray, $|Ang2|^{470} > 15°$, $r^2 = 0.92$) region of the male's visual field. n = 226 flies. **B**, Probability density of pulse production versus female angular location (Ang2) for WT (black, n = 226 flies) and half-blind (hBL, red, n = 15 flies) males. Light/dark red represent the unblocked/blocked regions of visual field. Line width indicates 95% confidence interval. **C**, Normalized amplitude versus Dis^{470} (bin width 0.2mm) for hBL males. Data was split into times when the female occupied the unblocked (light red, $-160° < Ang2^{470} < 15°$) or blocked (dark red, $15° < Ang2^{470} < 160°$) region of visual field. Dashed line indicates 5mm boundary, beyond which AMD was exclusively vision dependent. For Dis^{470} below and above 5mm, $r^2 = 0.97/0.54$, and $r^2 = 0.69/0.06$ for the unblocked/blocked region of space. n = 15 flies. **D**, Difference in normalized amplitude for pulses produced when female was in visual field *a* versus *b* for WT1 (black, n = 29 flies) and hBL (red, n = 14 flies). Flies sang > 50 pulses in each region. * $P < 0.01$. Individual flies, mean, and STD

are shown. **E**, Diagram of tethered fly-on-a-ball setup. Two microphones (blue rectangles) recorded song while an infrared laser heated the fly to activate subsets of song neurons (P1 or pIP10). Visual stimuli were presented at 144Hz. The horizontal (H) and vertical (V) stimulus dimensions, and the azimuthal motion (ΔAng2), varied according to the natural statistics of female motion on the male retina during courtship (see Experimental Procedures). Stimulus size was defined by the subtended angle of the stimulus at the fly's eye, divided into horizontal (hAng) and vertical (vAng) components. Ang2 represents the angular position of the stimulus on the male retina. **F**, Example of visual stimulus dynamics. Ang2 versus time for two different stimuli: **Top**, ΔV = ΔH. Ang2 ranges from −45° to +45° and hAng (green) is marginally smaller than vAng (blue, barely visible). **Bottom**, ΔV ≠ ΔH. hAng (green) and vAng (blue) vary independently. Line width indicates the size of the stimulus and arrows show example stimuli. **G**, Normalized amplitude versus stimulus size for $P1^{Act}$ males (n = 8) presented with naturalistic stimuli (ΔH = ΔV and $-45° < Ang2^{470} < 45°$). Activated males show AMD in response to this stimulus ($r^2 = 0.88/0.77$ for $hAng^{470}/vAng^{470}$). **H**, As In **G**, but for $pIP10^{Act}$ males (n = 8). $r^2 = 0.83/0.68$ for $hAng^{470}/vAng^{470}$. **H**, As in **G**, but without changes in azimuthal position (Ang2 = 0 and ΔH = ΔV). Neither $P1^{Act}$ (n = 6, $r^2 = 0.25$) nor $pIP10^{Act}$ (n = 6, $r^2 = \leq 0.02$) males showed AMD for this stimulus. **I**, As in **G**, but stimuli presented to $P1^{Act}$ (n = 6) and $pIP10^{Act}$ (n = 5) flies changed size independently for horizontal and vertical dimensions (ΔH ≠ ΔV and $-45° < Ang2^{470} < 45°$). Males did not show AMD in response to this stimulus ($r^2 = \leq 0.21$). **A**, **C–D**, and **F–J**, > 100 pulses contributed to each point. Error bars indicate SEM. **A–D** and **F–J**, All flies sang > 500 pulses. (See also Figure S6)

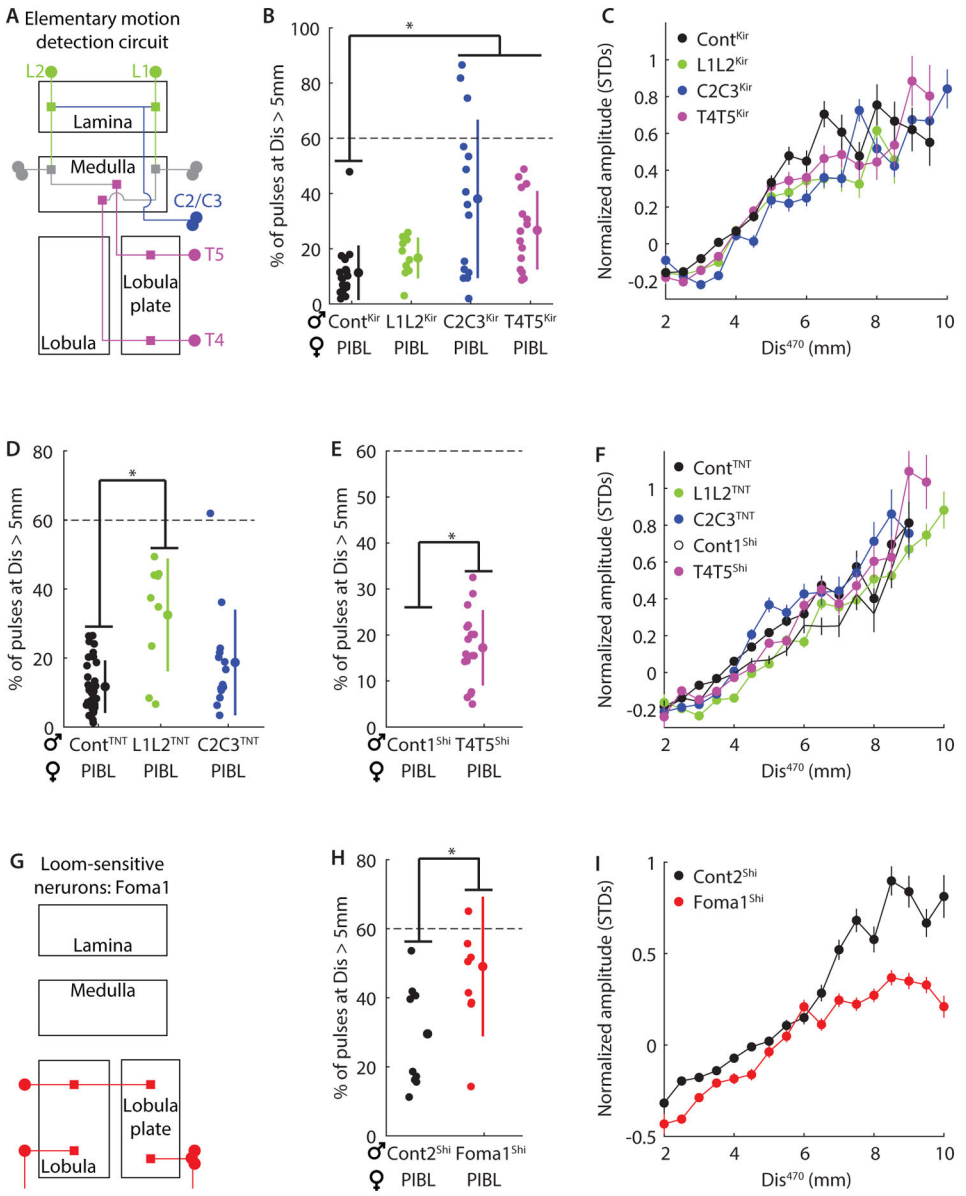

Figure 5. Motion- and loom-sensitive visual circuits are not required for AMD

A, Simplified diagram of the elementary motion detection (EMD) pathway. Three critical neural classes, silenced in pairs for this study, are labeled: lamina output neurons (L1 and L2), lamina feedback neurons (C2 and C3), and lobula plate columnar cells (T4 and T5). **B**, Ability of male to follow the female during courtship was quantified as the percentage of song pulses produced at distances > 5mm from the female. We observed following defects upon silencing EMD neural subsets with expression of inward-rectifying K+ channel (Kir) ($L1L2^{Kir}$, $C2C3^{Kir}$, and $T4T5^{Kir}$) compared with control flies ($Cont^{Kir}$; see Table S1 for genotypes). *P < 0.01, n = 11–22. **C**, However, AMD was unaltered: normalized amplitude versus Dis^{470} (bin width 0.5mm) for each strain from **B**, $r^2 \geq 0.81$, n = 11–21 flies. **D**, As in **B**, but for neural subsets silenced with tetanus toxin (TNT) ($L1L2^{TNT}$ and $C2C3^{TNT}$) compared to control flies ($Cont^{TNT}$). *P < 10^{-4}, n = 9–34. **E**, As in **B** but for neural subsets

silenced by expressing temperature-sensitive *shibire* at a non-permissive temperature ($T4T5^{Shi}$, ~28°C, n = 17) compared to control flies recorded at the permissive temperature ($Cont1^{Shi}$, ~22°C, n = 17) *P < 0.05. **F**, As in **C**, but using the strains from **D–E**, $r^2 \geq 0.86$. n = 8–34 flies. **G**, Schematic of the only identified loom-sensitive neurons (Foma-1). **H**, As in **E**, but for flies expressing $shibire^{TS}$ in loom-sensitive neurons at non-permissive ($Foma1^{shi}$) or permissive ($Cont2^{Shi}$) temperatures. **I**, As in **C**, but using the strains from **H**, $r^2 \geq 0.89$. n = 9–10 flies. **B**, **D**–**E,** and **H**, Individual flies, mean, and STD are shown. All flies sang > 250 pulses. Dashed line indicates mean fraction of pulses produced beyond 5mm for blind flies. **C, F**, and **I**, > 100 pulses contributed to each point and all flies sang > 500 pulses. Error bars indicate SEM. (See also Figure S7)

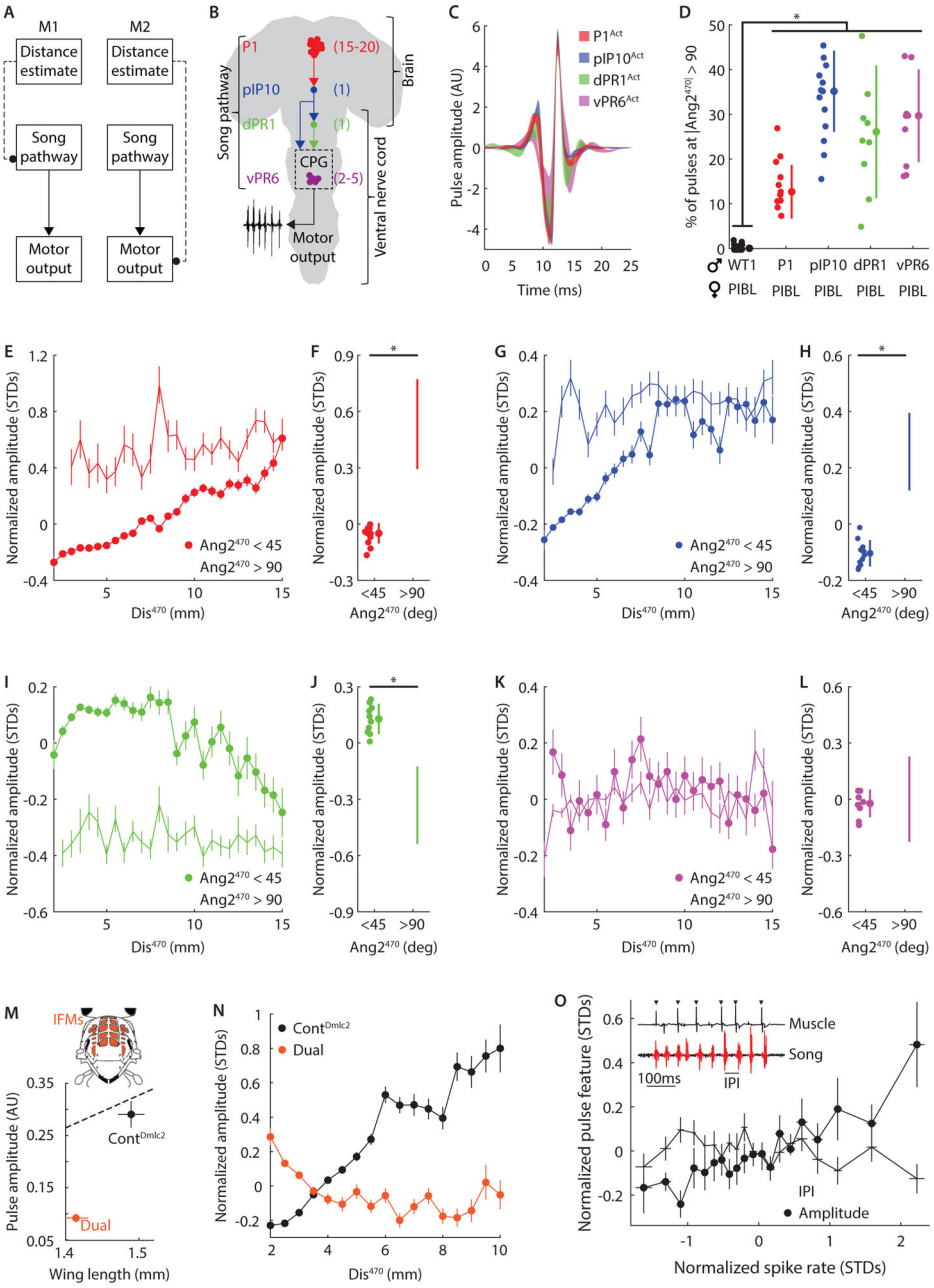

Figure 6. Descending visuomotor pathway

A, Diagram of alternative pathways for visual information (about distance to the female) interacting with the song motor pathway (at the level of the song pathway itself (M1) or directly with motor neurons or muscles (M2)). **B**, Diagram of the four previously identified components of the song circuit(von Philipsborn et al., 2011). Number of neurons in each hemisphere is indicated in parentheses. P1 neurons innervate the brain only, pIP10 is a descending neuron, while dPR1 and vPR6 neurons innervate the ventral nerve cord. vPR6 is thought to be integral to the pulse song central pattern generator (CPG). **C**, Shapes of "activated" pulses produced by males expressing TrpA1 (thermosensitive cation channel) in

the song neurons described in **B**. Shaded area indicates 95% confidence interval. **D**, Males with artificially activated song neurons produced more pulses when not facing the female than WT1 flies. *$P < 10^{-14}$, n = 8–39 flies. **E**, Normalized amplitude versus Dis^{470} (bin width 0.5mm) for $P1^{Act}$ males (n = 11) paired with PIBL females. AMD was observed when the males faced toward (closed circles, $r^2 = 0.95$) but not away from (open circles, $r^2 = 0.20$) females. **F**, $P1^{Act}$ males reduced pulse amplitude when facing the female. n = 11, *$P < 10^{-4}$. **G**, As in **E**, but for $pIP10^{Act}$ males (n = 12). AMD was observed when the males faced toward (closed circles, $r^2 = 0.76$) but not away from (open circles, $r^2 = 0.18$) the female. **H**, $pIP10^{Act}$ males reduced pulse amplitude when facing the female. n = 12, *$P < 10^{-5}$. **I**, As in **E**, but for $dPR1^{Act}$ males (n = 10). In contrast with PI^{Act} and $pIP10^{Act}$, pulse amplitude decreased with increasing Dis^{470} (opposite of AMD) when males faced toward (closed circles, $r^2 = 0.52$) but not away from (open circles, $r^2 = 0.08$) the female. **J**, $dPR1^{Act}$ males increased pulse amplitude when facing the female. n = 10, *$P < 10^{-4}$. **K**, As in **E**, but for $vPR6^{Act}$ males (n = 8). Pulse amplitude is independent of Dis^{470} whether males faced toward (closed circles, $r^2 = 0.16$) or away from (open circles, $r^2 = 0.06$) the female. **L**, $vPR6^{Act}$ males did not change pulse amplitude when facing the female. n = 10, *P > 0.81. **M**, *Dual* mutant males (orange) produced pulses of lower amplitude relative to matched controls (black). Error bars indicate SEM. Dashed line represents linear fit to wild type data (from Figure 1C). **Inset**, diagram of the indirect flight muscles (IFMs, orange). **N**, Normalized pulse amplitude versus Dis^{470} (bin width 0.5mm). AMD was observed for control (black, $r^2 = 0.93$) males, whereas *Dual* mutant males displayed a weak anti-correlation between Dis^{470} and amplitude ($r^2 = 0.44$). **O**, Simultaneous song and extracellular IFM recordings in $P1^{Act}$ males. For each song pulse, a corresponding spike rate was calculated over the preceding 5s and normalized for individual flies. Increased spike rates predict larger pulse amplitudes (closed circles, $r^2 = 0.81$) but are not correlated with the inter-pulse interval (open circles, $r^2 = 0.02$). n = 6 flies for each point. Error bars indicate SEM. **Inset**, raw song (bottom) and extracellular IFM recordings (top, triangles indicate identified spikes). **D**, **F**, **H**, **J**, and **L**, Individual flies, mean, and STD are shown. **E**, **G**, **I**, **K**, and **N**, > 100 pulses contributed to each point and all flies sang > 500 pulses. Error bars indicate SEM. **C–O**, All flies sang > 500 pulses. (See also Figures S1 and S8)

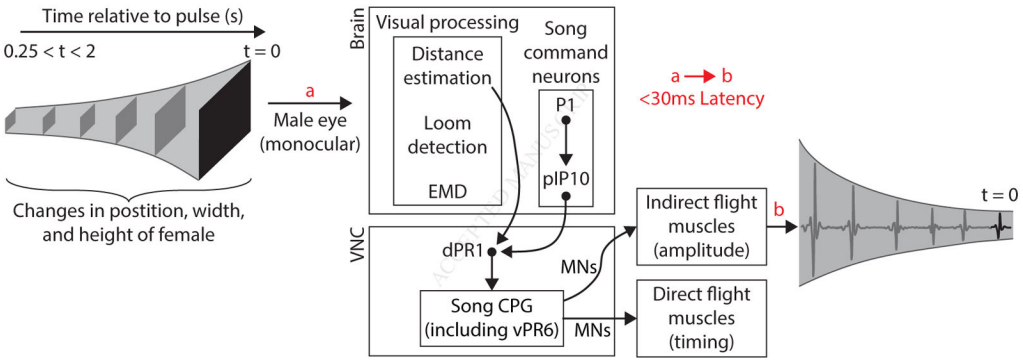

Figure 7. Proposed mechanism of AMD

Correlated changes in height and width, as well as lateral motion, of the female (black square) are processed through a monocular circuit in the male brain. Two-dimensional expansion information is extracted by a distance estimation pathway, which does not depend on either the identified elementary motion detection (EMD) or loom detection pathway. Distance information then intersects with the song motor pathway in the ventral nerve cord (VNC), downstream of song command neurons (P1 and pIP10). The song central pattern generator modulates the firing rate of motor neurons (MNs) that target the indirect flight muscles to adjust pulse amplitude. The latency between visual stimuli reaching the eye (a) and modulating pulse amplitude (b) is < 30ms, and visual stimulus history of < 2s, but > 250ms influences circuit output.